Electronic Supplementary Material (ESI) for Catalysis Science & Technology.

Electronic Supplementary Information

Embedded oxygen vacancies at SnO_2-CNT surfaces via microwave polyol strategy towards effective electrocatalytic reduction of carbon-dioxide to formate

Kumaravelu Pavithra[a] and Sakkarapalayam Murugesan Senthil Kumar, [*] [a,b]

[a] *Materials Electrochemistry Division, CSIR-Central Electrochemical Research Institute, Karaikudi, Tamil Nadu, 630 003, India,*

[b] *Acadamy of Scientific and Innovative Research (AcSIR), CSIR-Central Electrochemical Research Institute, Karaikudi, Tamil Nadu, 630 003, India.*

**Corresponding Author E-mail: senthilkumarsm@cecri.res.in; smsk_2k@yahoo.com*

Formulas used

1. Debye-Scherrer formula, $D = K\lambda / \beta \cos\theta$

   Where K= shape factor (0.89), λ= wavelength of the Cu-Kα radiation (1.5406 A°), β= full width at half maximum, cos θ = Bragg's angle of diffraction ($n\lambda = 2d \sin\theta$).

2. Faraday Efficiency (FE %) = nNF /Q * 100

   Where n = no. of moles of product, N = no. of electrons for a product, F = Faraday Constant, Q = Total charge during the reaction, FE = Faraday efficiency.

3. Energy Efficiency (EE %) = $FE(\%) * \Delta E^{\circ}_{HCOOH} / \Delta E_{HCOOH}$

   Where ΔE°_{HCOOH} = Difference in standard half reaction potential for water oxidation (1.23 V vs RHE) and CO_2 reduction to HCOOH (-0.2 V vs RHE) and ΔE_{HCOOH} =Difference in standard water oxidation potential and working potential of cathode.

4. Partial Current Density (PCD mA/cm^{-2}) = FE * Q/t * 1/A

   Where t = time, A= geometric area of electrode, PCD = partial current density

5. Turn over Number (TON) = Formate Product in mole/Catalyst loading in mol/cm^2 *geometric electrode area in cm^2

6. Turn over Frequency TOF(s^{-1}) =TON/Electrolysis time in sec

Supplementary Figures

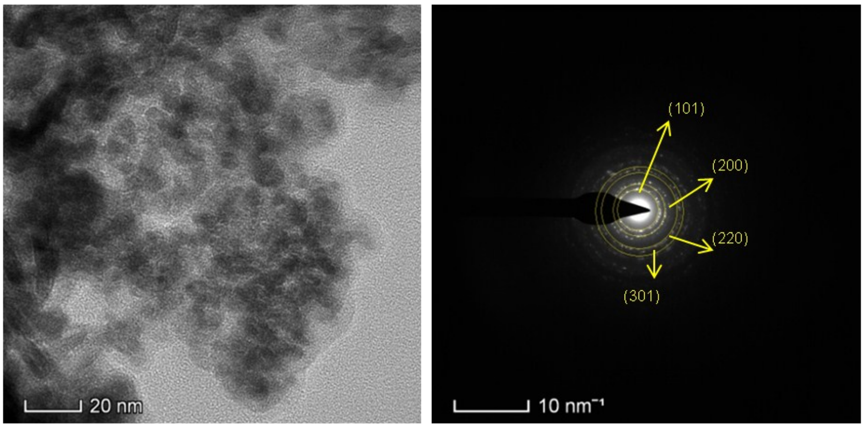

Fig. S1. HRTEM image of SnO_2 and its corresponding SAED pattern which is synthesised by using similar experimental procedure of Microwave polyol synthesis without adding CNT.

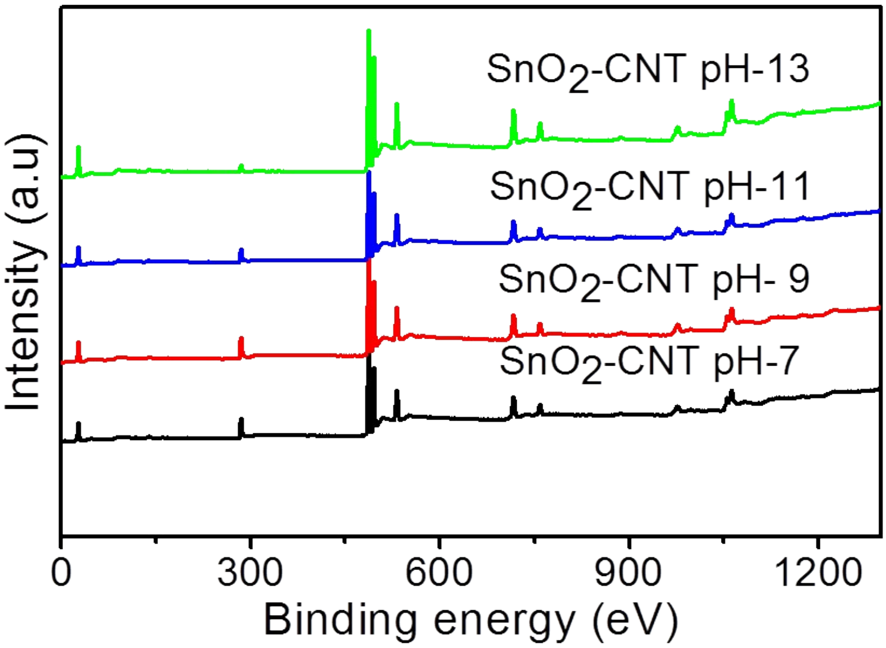

Fig. S2. Survey spectrum of all the synthesised SnO_2-CNT composites

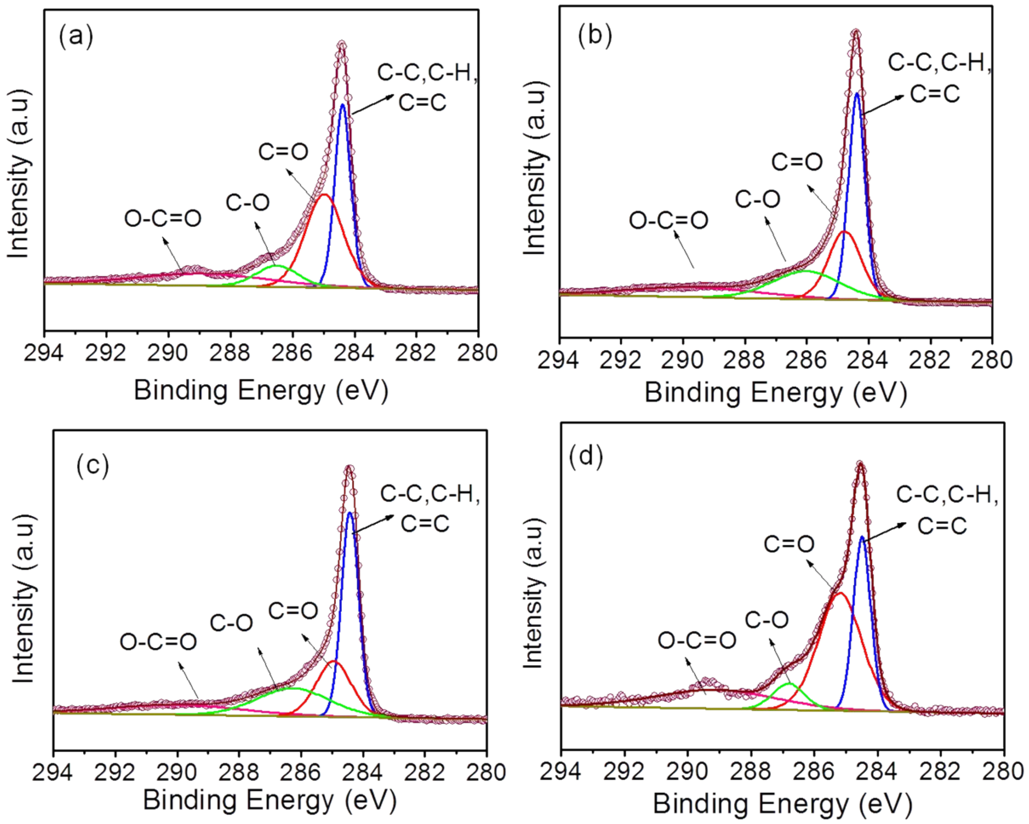

Fig. S3. (a), (b), (c) and (d) Deconvoluted spectrum of C 1s of SnO_2-CNT pH-7 , SnO_2-CNT pH-9, SnO_2-CNT pH-11, SnO_2-CNT pH-13 respectively

Mechanistic details

In order to understand the SnO_2-CNT formation mechanism, FT-IR was recorded in three different stages. The catalyst was collected at three different stages of the synthesis for example – (i) before microwave irridiation , (ii)after irradiation of microwave and (iii) after the calcinations step. In FT-IR, the peak around 1017, 1720, 2824 and 2920 cm^{-1} were attributed to –C-O, -C=O- and –CH- group from CNT. This confirms the presence of acid functionality in CNT. The peak at 1410 cm^{-1} is from the $–CH_2-$ of ethylene glycol. The broad peak around 3450 cm^{-1} is due to the presence of –OH from the surrounding water molecules. The appearance of vibrations at 1619 cm^{-1} indicates the presence of –Sn-OH bond. The formation of SnO_2 was confirmed by the presence O-Sn-O and Sn-O-Sn vibrations at 477 and 618 cm^{-1}. From the graph it is clearly seen that the nucleation has been initiated even before microwave irradiation. During microwave, the formation of SnO_2 occurs effectively. But still there is the presence of -Sn-OH and $-CH_2-$ vibrations which indicates incomplete reduction of Sn and the presence of ethylene glycol. After calcination, the ethylene glycol has been completely decomposed. During the deposition of SnO_2 on CNT surface, there is a significant decrease in the intensity of peaks corresponding to CNT confirms that the presence of acid functionality helps in anchoring SnO_2 on the surface of CNT. Our proposed mechanism based on FT-IR is in good agreement with XRD and Raman analysis

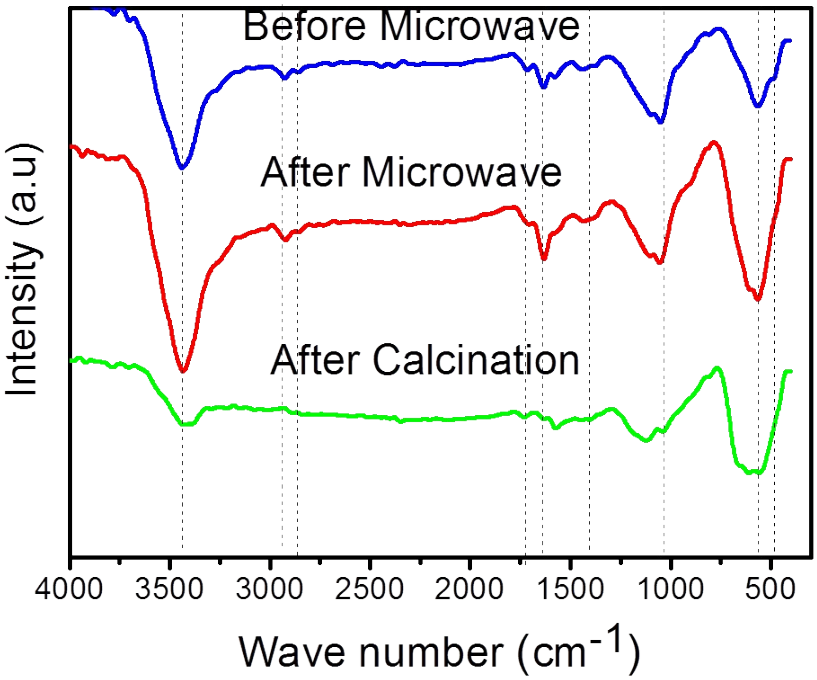

Fig. S4. FT-IR of SnO_2-CNT pH-11 at various stages of synthesis

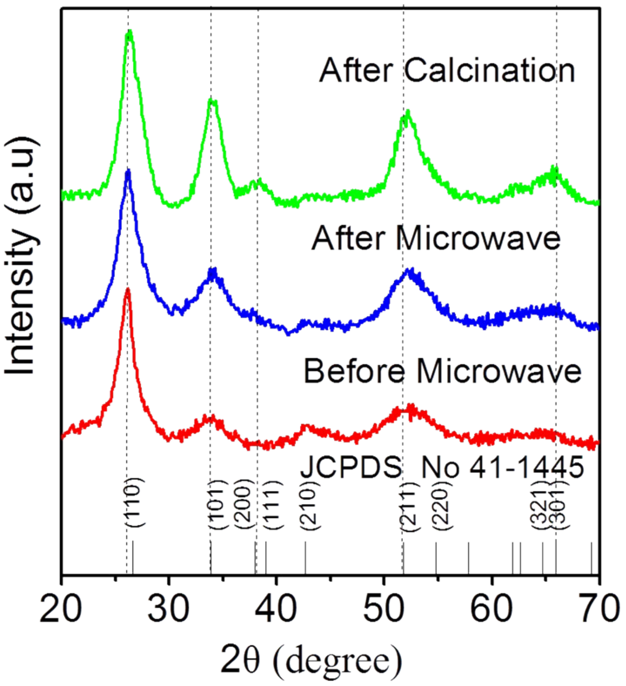

Fig. S5. XRD of SnO_2-CNT pH-11 at various stages of synthesis

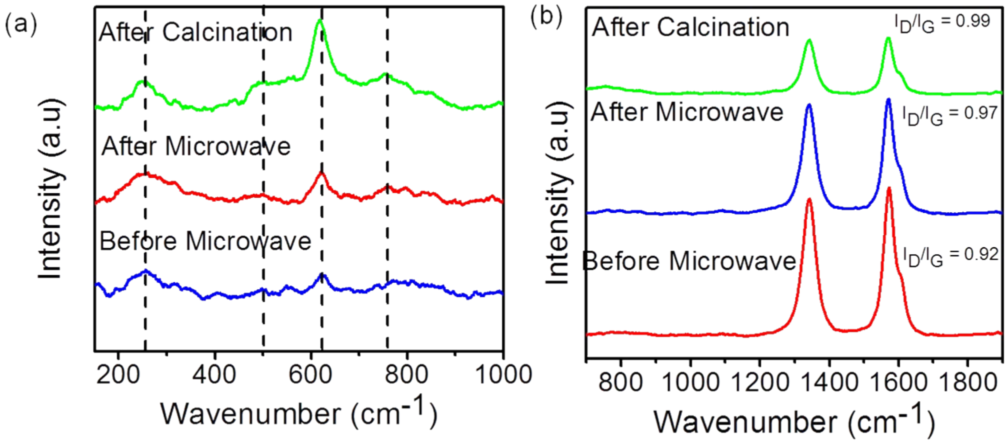

Fig. S6. (a) and (b) Raman spectra of SnO_2-CNT pH-11 at various stages of synthesis

Microwave induced oxygen vacancy

To understand the influence of microwave in oxygen vacancy, a control experiment was done. SnO_2-CNT pH-11 was synthesised in the presence and absence of microwave. The sample without microwave irradiation is labelled as pure SnO_2-CNT. The XRD and Sn 3d, O 1s of XPS spectra of as pure SnO_2-CNT confirms formation of SnO_2 with the absence of oxygen vacancy.

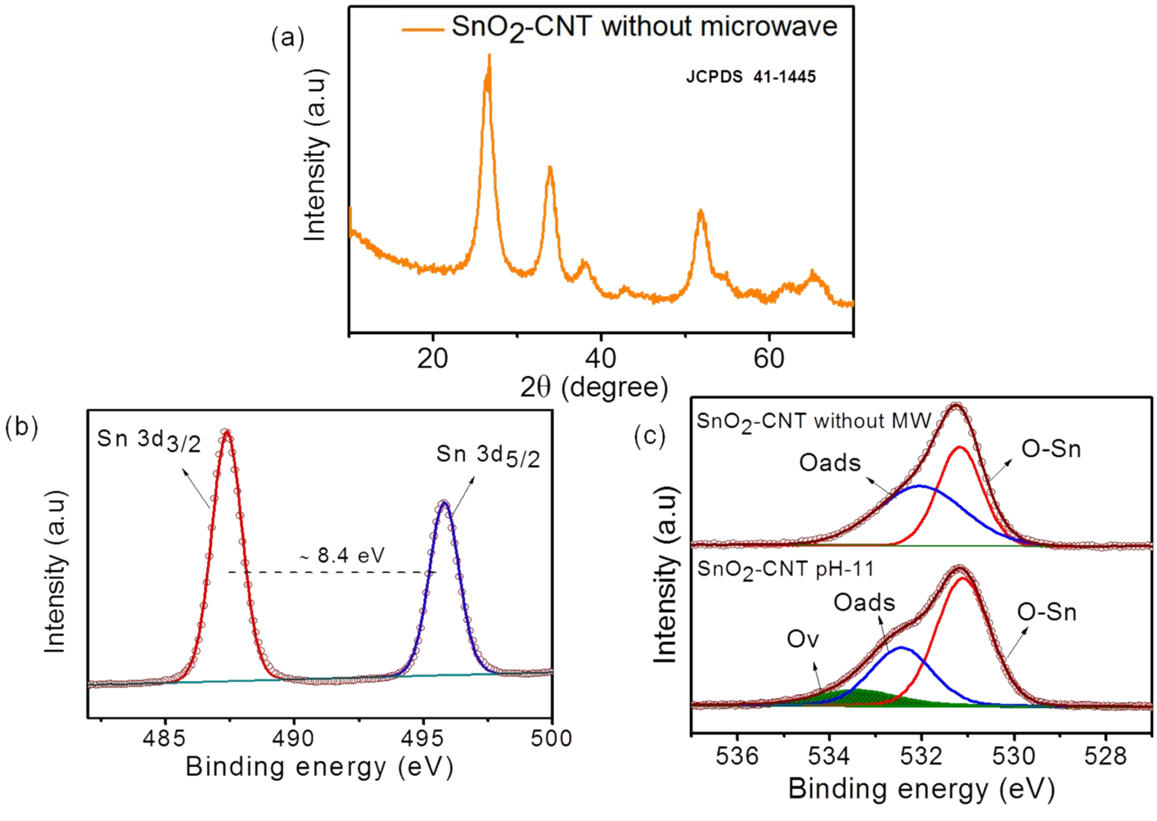

Fig. S7 (a) XRD spectrum of SnO_2-CNT without microwave (b) Sn 3d XPS spectrum of SnO_2-CNT without microwave (c) shows the O 1s spectra of pure SnO_2-CNT and SnO_2-CNT pH-11.

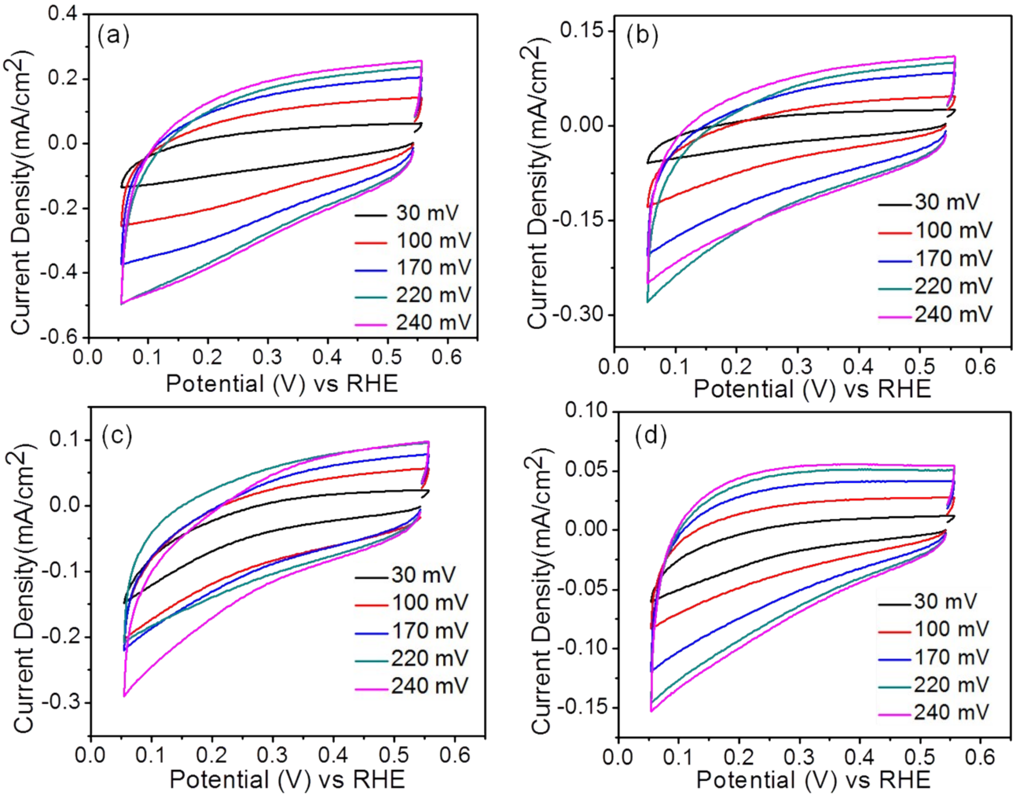

Fig. S8. (a), (b), (c) and (d) shows the capacitive behaviour of SnO_2-CNT pH-7 , SnO_2-CNT pH-9, SnO_2-CNT pH-11, SnO_2-CNT pH-13 respectively in the region of 0.05 to 0.55 V vs. RHE at different scan rates of 30, 100, 170, 220, 240 mV/sec in a 0.1 M K_2SO_4

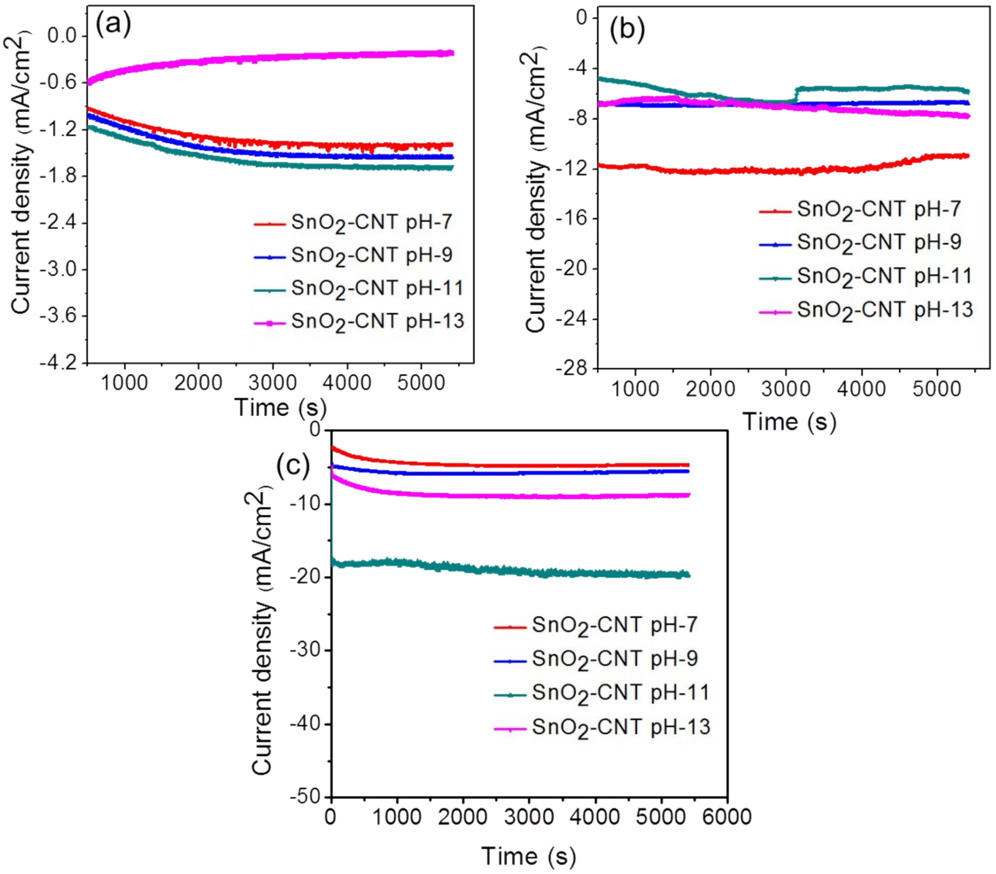

Fig. S9. (a), (b) and (c) Constant potential electrolysis plot of I vs. t for all the SnO_2-CNT composites at a fixed potential of -0.52 , -0.77 and -0.92 V vs. RHE respectively recorded over a time period of 5400 s. (provided only for one set of experiment)

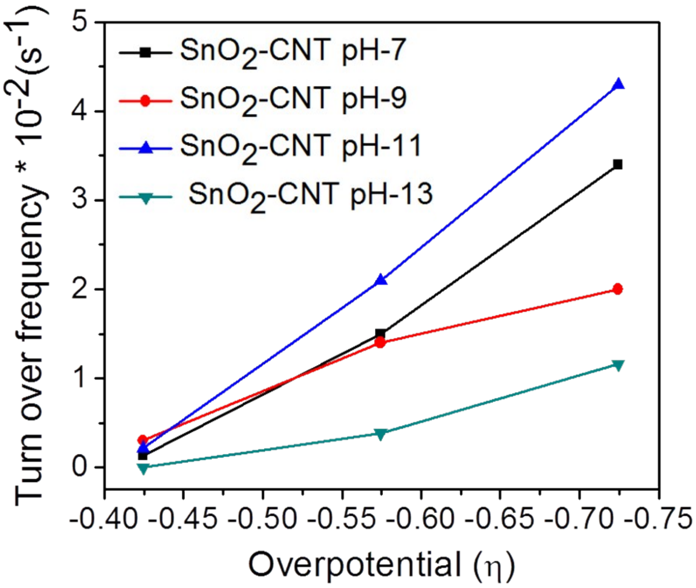

Fig. S10. depicts a plot of TOF change with respect to overpotential for all the composites.

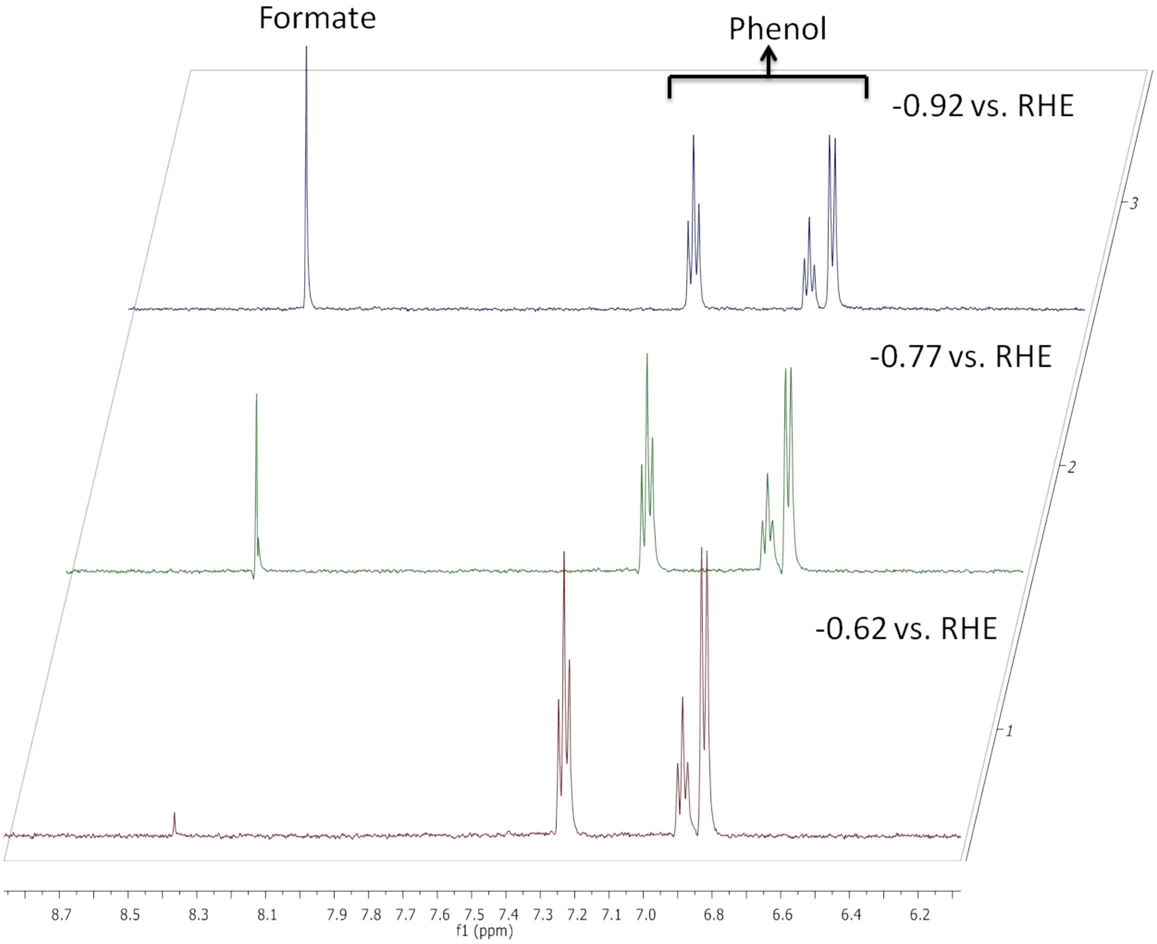

Fig. S11. ^{1}H NMR spectra of SnO_2-CNT pH-11 recorded in water suppression mode at -0.62, -0.77, -0.92 V vs. RHE which clearly indicates the presence of formate around 8.34 ppm along with phenol (internal standard) in the region of 6.8-7.3 ppm.

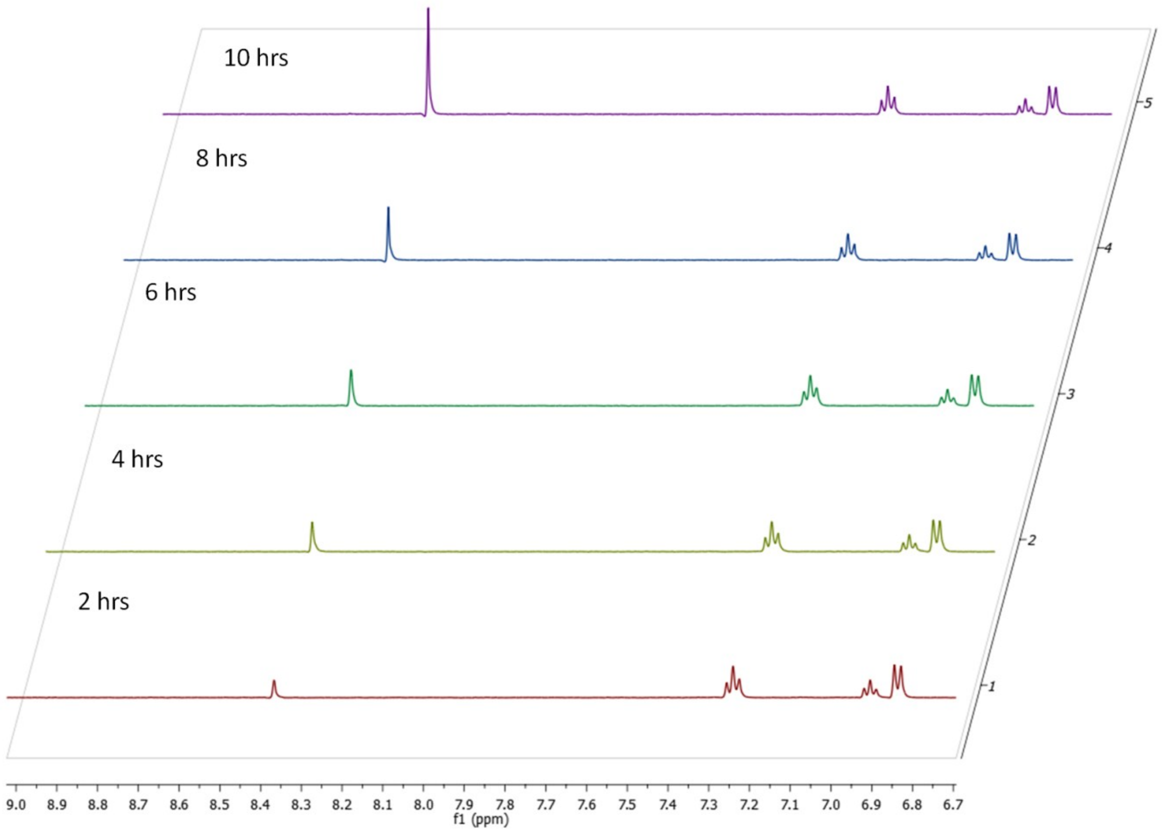

Fig. S12. ^{1}H NMR spectra of SnO_2-CNT (pH-11) recorded in water suppression mode at -0.77 vs. RHE at different time intervals.

Post-studies

SnO_2–CNT pH-11 catalyst was coated on a larger electrode area of 3 X 3 with the loading of 2 mg/cm^2 and subjected to bulk electrolysis at an applied potential of -0.77 V for about 5400 s. After electrolysis, the catalyst was removed from the carbon paper through sonication and post characterisation like XRD, XPS and EPR have been carried out. From XRD, it is quite clear that the SnO_2 rutile tetragonal phase has been retained even after electrolysis. Further Sn 3d XPS confirms the presence of Sn^{+4} with no other lower oxygen states like Sn/Sn^{+2}. This observation confirms the material stability. The retention of oxygen vacancy after electrolysis was confirmed by O 1s from XPS and EPR studies.

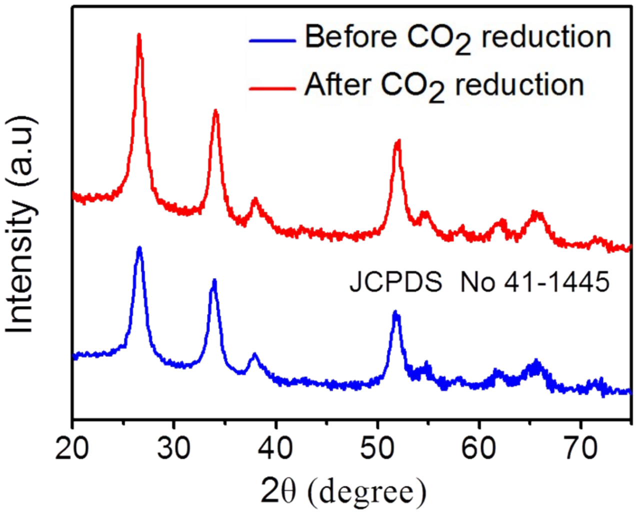

Fig. S13 XRD of SnO_2-CNT pH-11 before and after electrolysis at -0.77 V vs. RHE for about 5400 s

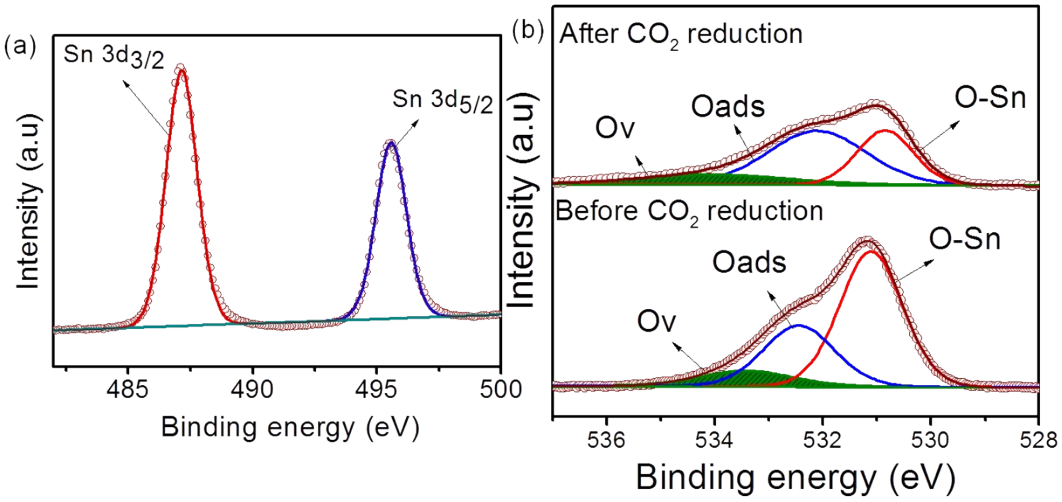

Fig. S14 Sn 3d XPS spectrum of SnO_2-CNT pH-11 after electrolysis at -0.77 V vs. RHE for about 5400 s (b) shows the O 1s spectra of SnO_2-CNT pH-11 before and after electrolysis at -0.77 V vs. RHE for about 5400 s.

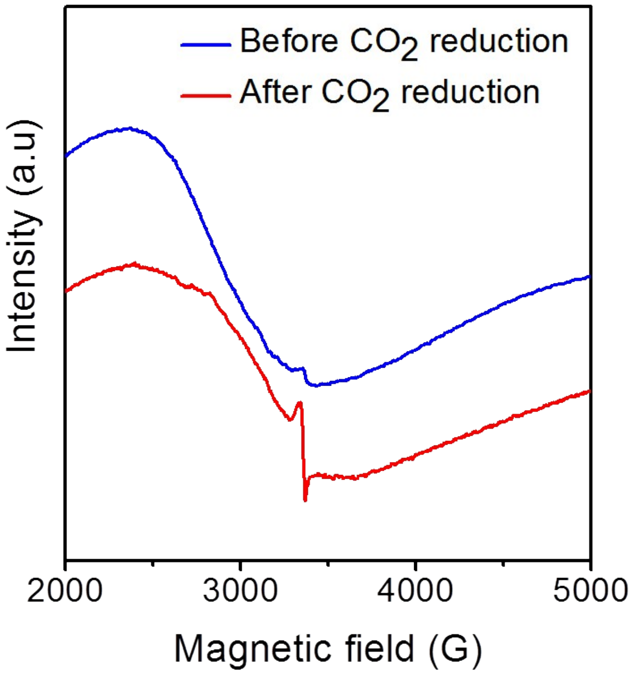

Fig. S15 EPR spectra of SnO_2-CNT pH-11 before and after electrolysis at -0.77 V vs. RHE for about 5400 s

Supplementary Tables

Table S1 depicts the comparison of electrocatalytic performance of our catalyst with the literature

Catalyst	**Area**	**Loading**	**Electrolyte**	**Potential (V)**	**Formate Faraday efficiency (%)**	**References**
SnO_2/C	0.5 cm _ 0.5 cm	-	0.1 M $KHCO_3$	-0.90 V vs RHE	54.00	*[3]*
SnO_2-CA-80	1.0 cm * 2.0	2.0 ± 0.2 mg/cm^2	1 M $KHCO_3$	-0.96 V vs RHE	76.00	*[4]*
SnO_2/CC	-	0.34 mg	0.5 M $NaHCO_3$	-1.60 vs. Ag/AgCl	87.00	*[5]*
N- SnO_2/C	-	-	0.5 M $NaHCO_3$	-0.65 V vs. RHE	90.00	*[6]*
SnO_2/Graphene	3 mm	2 mg cm^{-2}	0.1 M $NaHCO_3$	-1.16 V vs. RHE	93.60	*[7]*
20 % SnO_2-MWCNT	1 cm^2	30 mg cm^{-2}	0.5 M $NaHCO_3$	-1.7 V vs. SCE	27.20	*[8]*
SnO_2-MWCNT	-	20 mg cm^{-2}	0.1 M $KHCO_3$	-1.40 V vs. SCE	64.00	*[9]*
SnOx@MWCNT-COOH	4 (2×2) cm^2)	3 mg/cm^2	0.5 M $KHCO_3$	-1.25 V vs. RHE	77.00	*[10]*
SnO_2-0.14@N-rGO	1*1 cm^2	0.3 mg/cm^2	0.5 M $NaHCO_3$	-0.80 V vs. RHE	77.00	*[11]*
SnO_2-N doped CNT	3 mm	-	0.1 M $KHCO_3$	-1.30 V vs. Ag/AgCl	46.00	*[12]*
SnO_2/PC	1*1	1 mg/cm^2	0.5 M $KHCO_3$	-0.86 V vs. RHE	*92.00*	*[13]*
SnO_2-CNT (pH-11)	1*1	0.2 mg/cm^2	0.5 M $KHCO_3$	-0.77 V vs. RHE	75.00	This work

Table S2 depicts the comparison of synthetic methodology and electrocatalytic performance of our catalyst with the other catalyst with oxygen vacancy

Catalyst	**Methodology**	**Product**	**Potential (V) vs, RHE**	**Efficiency (%)**	**References**
Black reduced porous SnO_2	Heating at H_2 atm	Formate	-0.6 t0 -1.1	90.0	*[14]*
CuOx-Vo	Electrochemical reduction	C_2H_4	-1.4	63	*[15]*
CuO/In_2O_3	Different synthetic environment	CO	-0.895	85	*[16]*
m-SnO_2	Nanocasting method	Formate	-1.15	75	*[17]*
SnO_2	Flame spray pyrolysis	Formate	-1.1	85	*[18]*
Vo-rich Co_3O_4	Lamellar inorganic–organic hybrid intermediate strategy	Formate	-0.87 vs, SCE	85	*[19]*
ZnO	H_2 plasma treatment	CO	-1.1V	83	*[20]*
SnO_2-CNT	Microwave	Formate	-0.77	75	This work

References

1. *New J. Chem.,* 2018, **42**, 943—954.
2. Scientific Reports**,** 2019*,* **9**, 12935.
3. J. Mater. Chem. A, 2018, **6**, 20121–20127.
4. Appl. Catal. A Gen. 2017, **545** 159–166.
5. Angew. Chem. Int. Ed. 2017, **56**, 505 –509.
6. J. Energy Chem. 2017, **26**, 825–829.
7. J. Am. Chem. Soc. 2014, **136**, 1734−1737.
8. Journal of CO_2 Utilization 2016, **16** , 346–353.
9. Electrochemistry Communications 2016, 65, 9–13.
10. ChemSusChem. 2019, **12** 1443–1450.
11. Appl. Catal. B Environ. 2018, **239**, 441–449.
12. Materials Letters,2015, **141**,63–66.
13. J. Mater. Chem. A, 2019, **7**, 18428
14. Applied Catalysis B: Environmental 2020, **260**, 118134.
15. Small Methods **2018**, 1800449
16. Catal. Sci. Technol., 2019, DOI:10.1039/c9cy01396b
17. ACS Sustainable Chem. Eng. 2018, **6**, 1670−1679
18. Adv. Sci. **2019**, 1900678
19. Nature communications, 2017, **8**,14503.
20. Angew. Chem. Int. Ed. 2018, **57**, 6054 –6059.